**A FRACTAL ROUGH THERMAL MODEL FOR EMISSIVITY RETRIEVAL OF MERTIS LUNAR FLYBY SPECTRA.**

K. Wohlfarth[1], C. Wöhler[1], A. Grumpe[1], K. Bauch[2], M. D'Amore[3], H. Hiesinger[2], J. Helbert[3], A. Maturilli[3], A. Morlok[2], M. P. Reitze[2], N. Schmedemann[2], A. Stojic[2], I. Varatharajan[3], and I. Weber[2].
[1] Image Analysis Group, TU Dortmund University, Otto-Hahn-Str. 4, 44227 Dortmund, Germany (kay.wohlfarth@tu-dortmund.de), [2] Institut für Planetologie, Wilhelm-Klemm-Strasse 10, 48149, Germany, [3] Institute for Planetary Research, DLR, Rutherfordstrasse 2, 12489 Berlin, Germany.

**Introduction:** The BepiColombo mission is a joint project of the European Space Agency (ESA) and the Japan Aerospace Exploration Agency (JAXA). It started its seven year journey to planet Mercury on October 20th, 2018 [1]. During its journey, BepiColombo is guided towards the inner solar system by several gravity assist maneuvers and will be decelerated for orbit capture in December 2025 [1]. Among other instruments, the MErcury Radiometer and Thermal Infrared Spectrometer (MERTIS) of the Mercury Planetary Orbiter (MPO) acquires thermal infrared spectra at 7-14 µm during the flybys [2, 3]

To interpret the spectra of airless bodies, i.e., the Moon, and Mercury, emissivity has to be extracted from radiance measurements. In a laboratory setting, for a smooth surface or for observations of planetary bodies under small emission and incidence angles the emissivity of a sample is obtained by simply dividing the measured radiance by the Planck function for a single temperature value. However, airless planetary bodies such as Mercury, the Moon, and asteroids exhibit a substantial level of surface roughness that changes the thermal radiation, which may thus deviate significantly from a simple black body spectrum especially when observed under oblique illumination geometry. The radiation that is due to thermal emission is not a simple Planck function anymore but a non-linear superposition of many Planck functions with a unique mathematical structure. Consequently, surface roughness, self-heating, shadowing, and the spatial scales on which these effects occur, have to be considered. Various approaches to model surface roughness have been discussed before in the asteroid community [4,5] but also for planets and the Moon, e.g., [6].

Here, we present a thermal model that incorporates these effects based on fractal rough surfaces constrained with statistical properties of the Moon. We apply the model to the lunar spectra that were acquired by MERTIS on April 10th, 2020, to extract emissivity spectra. The model will also be used to calibrate the first flyby spectra of Mercury and telescopic measurements of Mercury in the near infrared [7].

**Methods:** We implemented a thermal roughness model of the Moon that partly builds upon [5], [8], [9] and [10]. There are also some similarities to [11]. The inputs of the model are the directional-hemispherical albedo $A_{dh}$, the incidence angle $i$ (measured between solar vector and surface normal), the emission angle $e$ (measured between view vector and surface normal), the azimuth $\varphi$ and the parameters for the roughness model. The map of $A_{dh}$ was derived from M³ data [9,12]. The output is the spectral radiance that is emitted by the surface for unit emissivity. The model follows three steps: First, we generate fractal random rough surfaces that reproduce the roughness properties of the lunar surface. [13] produced 3D models of the regolith based on stereo imagery that were obtained by the Apollo astronauts. They analyzed the 3D structure of the regolith on different scales, which serves as an input to our fractal rough surface routine. The rough surface model is slightly smoothed by a low-pass filter, such that the scales are reached at which isothermal behavior can be assumed. It has been shown by [6] and [9] that the Moon is isothermal on spatial scales of approximately 5 mm and above. This means that on these scales surface facets can be treated individually with negligible heat conduction on this scale. Secondly, we assume thermal equilibrium, so that the temperature of each facet is determined by the Stefan-Boltzmann law which depends on the facet's orientation toward the sun and $A_{dh}$ [10]. We implemented two ray-tracers that calculate the shadowing of the incident light and self-heating. Finally, the thermal emission of each facet is calculated with Planck's radiation law. The overall spectral radiance is the superposition of all Planck functions mitigated by the projection as described by [5]. Again, we use a ray-tracer to detect occlusions of the emerging beam. The emissivity is retrieved by dividing the measured radiance by the modeled thermal radiation.

**Application to MERTIS lunar flyby:** We simulated the lunar disk as seen by MERTIS at the time of the flyby. The disk was divided into 7800 pixels that are associated with the individual $A_{dh}$ values and the angles $i$, $e$ and $\varphi$. For each pixel, the thermal emission at

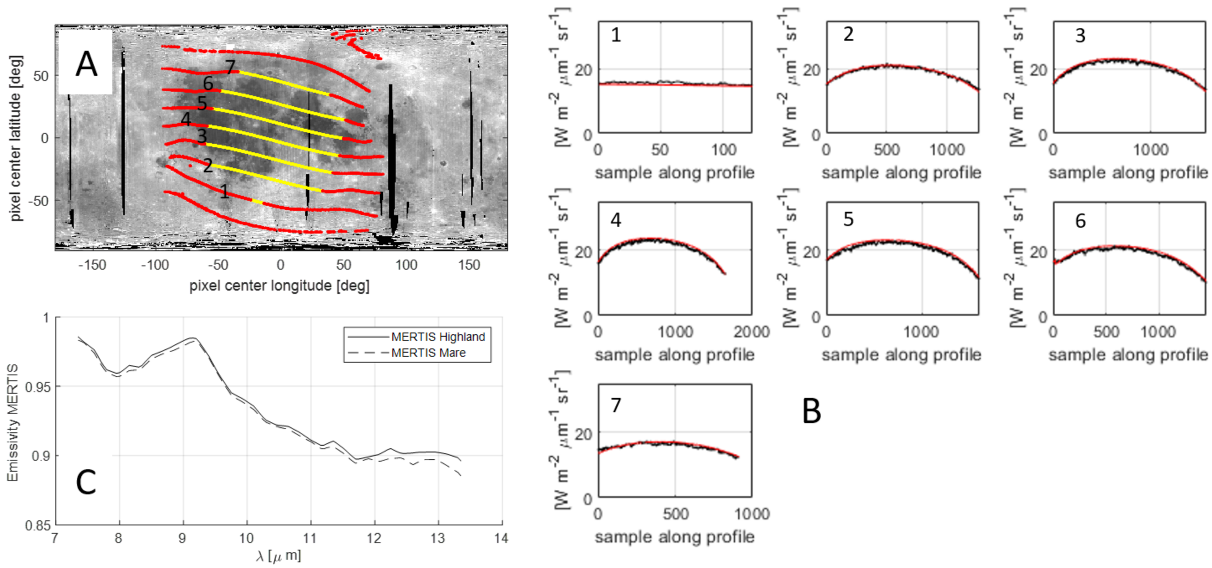


Figure 1. A: Tracks of MERTIS across the lunar disk. Background image: Moon Mineralogy Mapper ($M^3$) [15] reflectance at 1579 nm as derived by [16]. B: measured (black) and modeled (red) profiles @10.95 µm, which correspond to the yellow part of the tracks in A. C: Average emissivity of mare and highland regions, respectively. A pixel was designated as mare when the Fe content according to [17] at its center location exceeds 10 wt%.

unit emissivity is calculated based on a fractal rough surface of 500 x 500 pixels and an edge length of 1 mm. MERTIS acquired nine tracks across the lunar surface. The distance of BepiColombo to the Moon was comparatively large, such that the footprint of a MERTIS pixel is about 500 km x 500 km. A small offset between the nominal and the real pointing direction of MERTIS remained after the geometric correction described in [14] was performed. Further, the point spread function (PSF) of the instrument slightly blurs the emerging radiance and must be taken into account. To fine-tune the pointing offset and to match the PSF parameter, we applied a parameter identification routine that minimizes the root mean squared error between our radiance model and the measured data. However, our radiance model has a uniform emissivity of one, but the radiance that emerges from the Moon is modulated with the Moon's unique spectral emissivity spectrum that is not known in advance. This means that the emissivity that should be the result of the whole calibration procedure is needed to fine-tune the calibration. To address the coupling of these quantities, we employed an iterative optimization scheme that concurrently estimates the mean spectral emissivity of the lunar disk as well as the model parameters, i.e. the pointing offsets and the PSF parameter. To finally arrive at the calibrated emissivity for each location, each measured spectrum was divided by the modeled radiation at a given location.

**Results:** Figure 1A shows the locations of the radiance profiles that were obtained by MERTIS. The yellow positions only represent the first scan across the lunar disk and have been used exclusively for the geometric correction and emissivity extraction. Figure 1B compares measured and modeled radiances of our routine at 11.45 µm along the yellow part of the profiles. Note that our model can successfully reproduce the measurements, which is also the case for the full MERTIS wavelength domain. The average emissivity spectra of mare and highland after the final thermal calibration are shown in Figure 1C. It is remarkable that a strong maximum around 9 µm and a local minimum around 8 µm are present. The spectral interpretation of these features can be found in [18, 19].

**References**: [1] sci.esa.int/web/bepicolombo/-/60833-esa-pr-28-2018-bepicolombo-blasts-off-to-investigate-mercurys-mysteries [2] Helbert, J. et al. (2005) LPSC XXXVI, abstract #1753*,* 1151–1154. [3] Hiesinger et al. (2020) Space Sci. Review, 216, 110. [4] Delbo, M. et al. (2015) Asteroids IV. The University of Arizona Press, Tucson, AZ, pp. 107-128. [5] Davidsson, B.J. et al. (2015) Icarus, 252,1-21. [6] Bandfield, J. L. et al. (2015) Icarus 248, 357-372. [7] Varatharajan et al. (2021), this conference . [8] Rozitis, B. and Green, S. F. (2011) Monthly Notices of the Royal Astronomical Society 415(3), 2042-2062. [9] Grumpe, A. et al. (2019) Icarus 321,486-507. [10] Shkuratov et al. (2011) PSS, 59(13), 1326-1371. [11] Warren, T. J. et al. (2019) JGR 124 (2), 585-601. [12] Wöhler C. et al. (2017) *Sci. Adv.*, 3(9). [13] Helfenstein, P. and Shepard, M. K. (1999) Icarus 141 (1), 107-131. [14] Schmedemann et al. (2021), this conference. [15] Green et al. (2011) JGR Planets, Vol. 116, E10. [16] Wöhler et al. (2014) Icarus 235, 86-122. [17] Bhatt, M. et al. (2019) A&A 627, A155. [18] Morlok et al. (2021), this conference. [19] Wohlfarth et al. (2021), this conference.